

# UWB PULSE GENERATION FOR GPR APPLICATIONS

*Thesis submitted in partial fulfillment  
of the requirements for the degree  
of*

Master of Technology

*by*

**ANIL KUMAR MANDALANKA**

*Roll no-211EC3313*

*under the guidance of*

**PROF. SUBRATA MAITI**



Department of Electronics and Communication Engineering  
National Institute of Technology, Rourkela  
Odisha, 769 008, India



Department of Electronics and Communication Engineering  
**National Institute of Technology Rourkela**  
Rourkela-769 008, Odisha, India.

Date

## Certificate

This is to certify that the thesis entitled, “**UWB PULSE GENERATION FOR GPR APPLICATIONS**” submitted by **Mr. ANIL KUMAR MANDALANKA** in partial fulfillment of the requirements for the award of Master of Technology Degree in Electronics and Communication Engineering with specialization in “**Electronics and Instrumentation**” during session 2012-2013 at the National Institute of Technology, Rourkela (Deemed University) is an authentic work carried out by him under my supervision and guidance. To the best of my knowledge, the matter embodied in the thesis has not been submitted to any other University/ Institute for the award of any degree or diploma.

**Prof. Subrata Maiti**

## Acknowledgement

This project is by far the most significant accomplishment in my life and it would be impossible without people who supported me and believed in me.

I would like to extend my gratitude and my sincere thanks to my honorable, esteemed supervisor **Prof. SUBRATA MAITI**. He is not only a great teacher/professor with deep vision but also and most importantly a kind person. I sincerely thank for his exemplary guidance and encouragement. His trust and support inspired me in the most important moments of making right decisions and I am glad to work with him. My special thank goes to **Prof. S. Meher** Head of the Department of Electronics and Communication Engineering, NIT, Rourkela, for providing us with best facilities in the Department and his timely suggestions.

I want to thank all my teachers **Prof. S. K. Patra, Prof. K. K. Mahapatra, Prof. U. C. Pati, Prof. T. K. Dan, Prof. S. K. DAS** and **Prof. L. P. ROY** for providing a solid background for my studies and research thereafter. They have been great sources of inspiration to me and I thank them from the bottom of my heart.

I would like to thank all my friends and especially my classmates for all the thoughtful and mind stimulating discussions we had, which prompted us to think beyond the obvious. I have enjoyed their companionship so much during my stay at NIT, Rourkela. I would like to thank all those who made my stay in Rourkela an unforgettable and rewarding experience. Last but not least I would like to thank my parents, who taught me the value of hard work by their own example. They rendered me enormous support during the whole tenure of my stay in NIT Rourkela.

*ANIL KUMAR MANDALANKA*

# Abstract

In this work, we present a low-complexity, and low cost ultra-wideband (UWB) pulse generators for GPR applications. Here we have implemented two UWB pulse generator circuits. The first pulse generator uses a simple common emitter amplifier followed by RC high-pass filter to generate the Gaussian pulse directly. The circuit provides a Gaussian pulse when activated by a square wave of an external trigger signal and also the pulse width duration tunability by varying the frequency. Using this circuit topology we can achieve 200ns Gaussian pulse. The second UWB pulse generator is based on the avalanche transistor. This pulse generator also provides a Gaussian pulse when activated by a square wave of an external trigger signal. And when activated with 3 kHz square wave, it generates 11ns duration Gaussian pulse.

# Contents

<b>1</b>	<b>Ground Penetrating Radar</b>	<b>2</b>
1.1	Introduction . . . . .	2
1.2	GPR History . . . . .	2
1.3	Applications . . . . .	4
1.4	GPR Principle . . . . .	4
1.5	Description of a time domain GPR . . . . .	7
1.5.1	Transmitter . . . . .	7
1.5.2	Receiver . . . . .	8
1.5.3	Timing circuit . . . . .	10
1.6	Problems areas . . . . .	10
1.7	Goal of the thesis . . . . .	11
1.8	Conclusion . . . . .	11
<b>2</b>	<b>UWB Pulse Generation Technology</b>	<b>12</b>
2.1	Introduction . . . . .	12
2.2	Types of UWB pulses popularly used in GPR . . . . .	14
2.3	Fundamentals of Pulse Generation Techniques . . . . .	15
2.3.1	Transmission line based Pulse Generators . . . . .	16
2.3.2	CMOS based UWB Pulse Generators . . . . .	21
2.4	Methods to approach: . . . . .	30
2.5	Summary and Conclusion: . . . . .	32
<b>3</b>	<b>IMPLEMENTATION OF THE PULSE GENERATOR CIRCUITS</b>	<b>33</b>
3.1	Introduction . . . . .	33
3.2	Transistor based UWB pulse generator . . . . .	33
3.2.1	Conclusion . . . . .	36
3.3	Avalanche transistor based UWB pulse generator . . . . .	36

---

3.3.1	Conclusion . . . . .	39
<b>4</b>	<b>Summary and Conclusion</b>	<b>40</b>
4.1	Summary . . . . .	40
4.2	Scope of the future work . . . . .	40
4.3	Conclusion . . . . .	41
	<b>BIBLIOGRAPHY</b>	<b>42</b>

# List of Figures

1.1	Ground Penetrating Radar block diagram. . . . .	5
1.2	Typical signal, received by the GPR. . . . .	5
1.3	Block diagram of a time domain GPR. . . . .	8
1.4	Block diagram of receiver. . . . .	8
1.5	Gain curve as a function of time. . . . .	10
2.1	Gaussian pulse. . . . .	13
2.2	Gaussian monocycle pulse. . . . .	13
2.3	Double differentiated Gaussian pulse. . . . .	14
2.4	Gaussian pulse generator using a fast step generator and transmission lines. .	16
2.5	Schematic of the new monocycle pulse generator. . . . .	18
2.6	Circuit of the monocycle-pulse generator. . . . .	19
2.7	Schematic of a SRD pulse generator. . . . .	20
2.8	Schematic of the pulse generation circuit. . . . .	21
2.9	Heterodyning for pulse generation. . . . .	23
2.10	Alternative time gating for pulse generation. . . . .	24
2.11	Filtering for pulse generation. . . . .	25
2.12	RLC pulse shaping circuit as a second-order differentiator. . . . .	26
2.13	Digital logic for impulse generator. . . . .	26
2.14	Baseband impulse combination for UWB pulse generation. . . . .	28
2.15	Trigger edge combination for UWB pulse generation. . . . .	29
2.16	Direct digital waveform synthesis for UWB pulse generation. . . . .	29
2.17	BJT based Pulse generator architecture. . . . .	31
2.18	Control Signals and generated Gaussian pulse. . . . .	31
2.19	Avalanche transistor UWB pulse generator. . . . .	31
3.1	Gaussian Pulse Generator and Control Signals. . . . .	34

---

3.2	Simulated Result. . . . .	34
3.3	Photo of the Implemented UWB Gaussian pulse generator on Breadboard. .	35
3.4	Photo of the OUTPUT of the Implemented UWB Gaussian Pulse Generator.	35
3.5	UWB pulse Generator using avalanche transistor . . . . .	37
3.6	simulated output of avalanche circuit . . . . .	37
3.7	Bench setup of the circuit . . . . .	38
3.8	Implemented circuit . . . . .	38
3.9	Output of the implemented circuit . . . . .	39



# List of Tables

3.1	Summary of BJT Based UWB pulse generator circuit . . . . .	36
3.2	Summary of Avalanche Transistor Based UWB pulse generator circuit . . . .	39

# Chapter 1

## Ground Penetrating Radar

### 1.1 Introduction

Ground Penetrating Radar belongs to the family of radar systems that image the sub-surface. GPR is also called as Surface Penetrating Radar (SPR). Nowadays, GPR is a fast growing technology and the number of its applications is still growing. Locating pipes and cables, civil engineering (bridge inspection, finding voids), security, archeology investigation, geophysical survey and ice mapping are a few examples of its application. The operating principle of GPR is based on Maxwell's equation of EM wave propagation in inhomogeneous sub-surface media. It couples EM waves in the ground and samples the backscattered echoes. The EM wave will be backscattered based on any electrical parameters contrasts in the ground. The special property of GPR is that it can detect echoes due to all three types of electrical parameters contrasts, i.e. electric resistivity( $\varepsilon_r$ ), magnetic permeability( $\mu_r$ ) and conductivity( $\sigma$ ). This means that a GPR system has potential for locating and identifying both metallic and non-metallic buried targets based on the echo characteristics. [21].

### 1.2 GPR History

In 1904 Hulsmeier first used the electromagnetic signal to determine the presence of remote terrestrial metal objects, but six years later description of their use for location of buried objects came into sight in a German patent by Leimbach and Lowy. Their technique consisted of burying dipole antennas in an array of vertical boreholes and comparing the magnitude of signals received when successive pairs were used to transmit and receive. In this way, a crude image could be formed of any region within the array which, through its higher

conductivity than the surrounding medium, preferentially absorbed the radiation. These authors described an alternative technique, which used separate, surface-mounted antennas to detect the reflection from a sub-surface interface due to ground water or to an ore deposit.

An extension of the technique led to an indication of the depth of a buried interface, through an examination of the interference between the reflected wave and that which leaked directly between the antennas over the ground surface. CW operation, uses shielding or diffraction effects due to underground features, and the reliance on conductivity variations to produce scattering, were present in a number of other patent disclosures, including some intended for totally submerged applications in mines. Pulsed techniques to determine the structure of buried features is first used by Hollenbeck [6], In 1926 it Come into sight. He noted that any dielectric variation, not necessarily involving conductivity, would also produce reflections and that the technique, through the easier realisation of directional sources, had advantages over seismic methods[4]. From 1930s onwards Pulsed techniques were developed as a means of probing to considerable depths in ice[7, 22], fresh water, salt deposits[23], desert sand and rock formations[11, 15]. Probing of rock and coal was also investigated by cook [2, 3], and Roe and Eller Bruch[18], although the higher attenuation in the latter material meant that depths greater than a few metres were impractical. A more extended account of the history of GPR and its growth up to the mid-1970s is given by Nilsson [16].

In the early 1970s when lunar investigations and landing were in progress interest about this subject is increased. Ground penetrating radar has advantage than seismic techniques was exploited, namely the ability to use remote, non-contacting transducers of the radiated energy, rather than the ground contacting types needed for seismic investigations. The dielectric impedance ratio between free space and soil materials, typically from 2 to 4, is very much less than the corresponding ratio for acoustic impedances, by a factor which is typically of the order of 100, so it is possible to use remote transducers[4]. From the 1970s until the present day, the range of applications is increasing very much. Now it includes building and structural non-destructive testing, archaeology, road and tunnel quality assessment, location of voids and containers, tunnels and mineshafts, pipe and cable detection, as well as remote sensing by satellite. Nowadays user has a better choice of equipment and techniques because for each application purpose built equipment is developed.

## 1.3 Applications

Recent progress has been one of continuing technical advance largely applications driven, but as the requirements have become more demanding, so the equipment, techniques and data processing methods have been developed and refined.

- GPR has been used in the following applications:
- Archaeological investigations
- Borehole inspection
- Bridge deck analysis
- Building condition assessment
- Contaminated land investigation
- Detection of buried mines(anti-personnel and anti-tank)
- Evaluation of reinforced concrete
- Forensic investigations
- Geophysical investigations
- Medical imaging
- Pipes and cable detection
- Planetary exploration
- Tunnel linings.

## 1.4 GPR Principle

Nowadays Ground Penetrating Radar (GPR) is one of the most promising technologies for close detection and identification of buried Anti-Personnel (AP) Landmines, due to its ability of detecting non-metallic objects in the sub-surface. The operating principle of Ground Penetrating Radar is it sends the EM waves into the ground and samples the backscattered echoes. The EM wave will be back scattered on any electrical parameters change in the

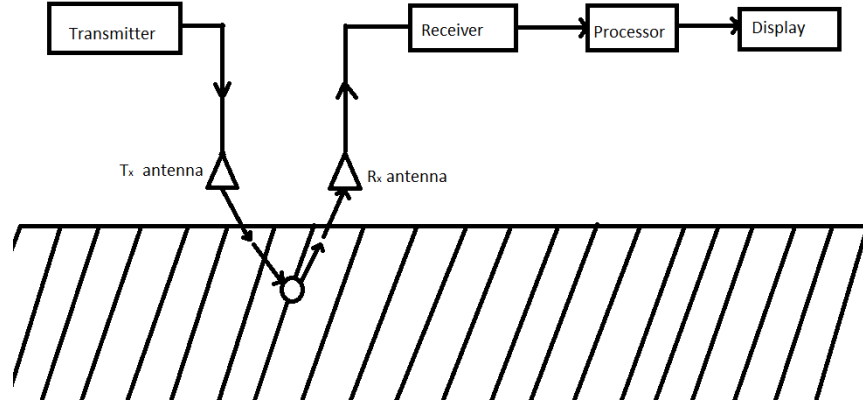


Figure 1.1: Ground Penetrating Radar block diagram.

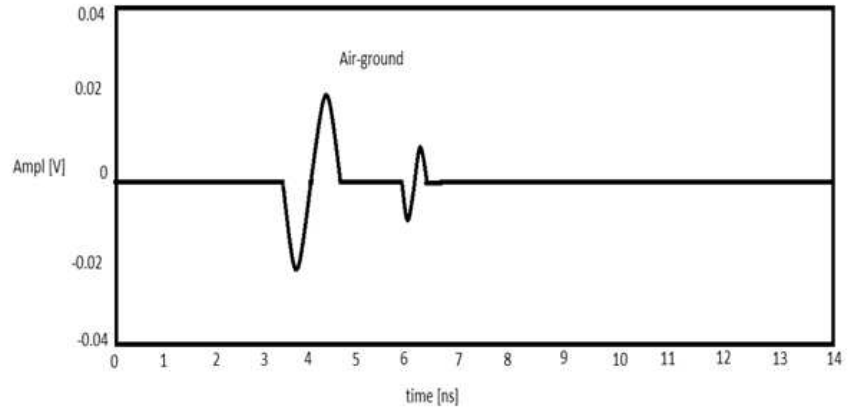


Figure 1.2: Typical signal, received by the GPR.

ground. The property of the GPR is that it can detect echoes from all three types of electrical parameters contrasts, i.e.  $(\epsilon_r)$ ,  $(\mu_r)$  and  $(\sigma)$ . This property telling that the GPR system has potential for locating and identifying both metallic and non-metallic buried targets on the echo characteristics[13].

Figure.1.1 shows a block diagram of a generic GPR system. In GPR the antennas are normally scanned over the surface in close to the ground. An EM wave sent into the ground will backscatter on any electrical parameter discontinuity. The backscattered echoes that reach the receiving antenna are sampled and processed by a receiver.

Figure 1.2 shows a typical time representation of a signal, received by the GPR at a given fixed position. Normally the first and the largest echo are due to the air-ground interface and other echoes, appearing later in time are reflections on target or clutter present in

the subsurface[3]. The GPR can produce two or three-dimensional images by moving the antennas on a line or a two dimensional grid. The main difference between the GPR and metal detector is, the GPR has the potential to detecting non-metallic targets also in the application of AP land mine detection.

Ground Penetrating Radar can be classified as below.

- Time Domain GPR
  - amplitude modulated GPR
  - carrier free GPR
- Frequency Domain GPR
  - Linear Sweep GPR
  - Stepped Frequency GPR

The first family of GPR systems is the time domain GPR. Time domain GPR is divided into two categories: the amplitude modulated and the carrier free GPR. The time domain GPR principle is it send a pulse at a given pulse repetition frequency (PRF) into the ground and then receives the backscattered echoes.

The amplitude modulated GPR sends a pulse with a carrier frequency. This carrier frequency is modulated by a square envelope. For good depth resolution it is important that the duration of the pulse is as short as possible. So a mono cycle is used. Mono cycle central frequency can vary from some MHz up to some GHz as a function of the application. Here the 3dB bandwidth of the emitted pulse is equal to the central frequency  $f_c$  of the mono cycle.

The need for larger bandwidth has led to the development of a second category of time domain GPR i.e. carrier free GPR. This GPR sends pulse without carrier. The width of the carrier free pulse is of the order of some 100 ps. In this GPR we can any type of pulse but typically a Gaussian pulse used. The carrier free GPR is also called an **UWB GPR**.

The second family of GPR system is Frequency Domain GPR. This is divided into two major categories: linear sweep GPR and stepped frequency GPR. In the first category continuous wave is frequency modulated with a linear sweep, named FMCW GPR. In the

second category the frequency of the continuous wave changes in fixed steps, called stepped frequency GPR[19].

A FMCW GPR system continuously transmits a changing carrier frequency by means of a VCO over a chosen frequency range. The frequency sweeps according to a saw-tooth or a triangular function within a certain dwell time. The receiver receives the backscattered signal and mixed with the emitted wave. The frequency difference between the transmitted and received wave is a function of the depth of the target. The main drawback of FMCW radar is the poor dynamic range of the system. The FMCW radar simultaneously receives the signals and transmits the signals. The leakage signal between the antennas can mask the smaller backscattered signals. Because of this the development of FMCW for the GPR application is decreased and from the late 1970's on, more attention has gone to the stepped-frequency radar[19].

A stepped frequency GPR uses a frequency synthesizer to step through a range of frequencies equally spaced by an interval  $\Delta f$ . Here a CW is radiated with a high stability and mixed with the received signal at each frequency using a quadrature mixer. By using high precision and low speed A/D converters, the I and Q baseband signals are sampled. Because of this at each frequency, the amplitude and phase of the received signal is compared with the transmitted signal. We can find more details about this in [1, 19].

## 1.5 Description of a time domain GPR

Besides of the data processing and display the time domain GPR has the three major parts: transmitter, timing circuit and receiver unit. Here the timing circuit triggers both the transmitter and receiver. The block diagram of the time domain GPR is shown in figure 1.3.

### 1.5.1 Transmitter

The transmitter is a pulse generator, it produces short transient pulses with a certain periodicity. This periodicity is called the pulse repetition frequency (PRF). In this GPR the shape of the pulse is typically a mono cycle or a Gaussian pulse, but we can use other shapes also like a derivative of a Gaussian pulse or even a step are possible. The technique of the impulse generator is generally based on rapid discharge of stored energy in a capacitor

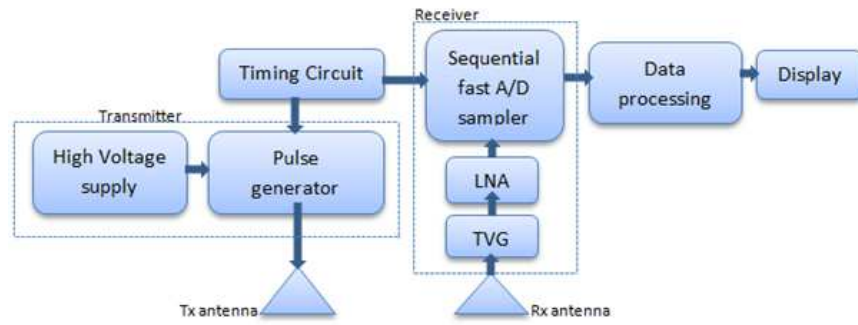


Figure 1.3: Block diagram of a time domain GPR.

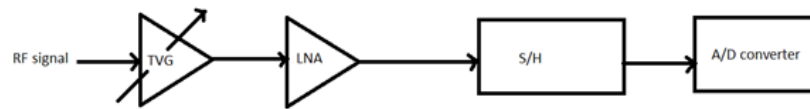


Figure 1.4: Block diagram of receiver.

or short transmission line.

### 1.5.2 Receiver

The receiver is the most difficult block in the hardware to build. Its performance has a direct impact on the over-all system performance. The receiver has to be very sensitive, possess a large fractional bandwidth, a large dynamic range and a good noise performance. The receiver have the four main blocks: a time-varying gain (TVG) amplifier, a low noise amplifier (LNA), a sample and hold circuit (S/H), and an analog-to-digital converter (A/D converter). The block diagram of receiver is shown in figure 1.4.

#### A/D converter

The signal received by the GPR systems is in the frequency range of some GHz, so it is impossible to use a standard A/D converter to sample the received echoes in real time, in order to respect Shannon's theorem. The solution to this problem is sequential sampling technique.



### Sample and hold circuit

The input to the A/D converter has to be stable for a certain time for a correct A/D conversion. The principle is that the maximum rate of signal variation must be smaller than the quantization step of the converter during the conversion time. Here a sample and hold (S/H) circuit is used to provide a constant signal value to the A/D converter. The working principle of a S/H circuit is based on the charging of a capacitor  $C_s$  to a voltage that is proportional to the input signal so that the sample corresponds to a specific portion of the input signal.

### The low noise amplifier (LNA)

Before the RF signal enters the S/H circuit, it is conditioned to make use of the whole Dynamic range of the A/D converter. Here the LNA i.e. an amplifier with a very low noise figure is the part of the signal conditioning elements. As shown in the GPR receiver, as represented in Fig. 2-17, is the correct order of succession of the elements. The LNA is not put as first element as one can expect, but after the TVG. We can see the explanation for this sequence in the utility of the time varying gain.

### Time varying gain (TVG)

The transmitting antenna radiates the spherical waves, that waves and the backscattered signal by an object are both subject to spreading loss. This means that in the far field the amplitude of the received echo of a given target decreases with  $R^{-2}$ , where  $R$  is the one-way path between the antennas and the object. And the objects that we are looking for are buried in a lossy medium. The deeper the object is buried, the more losses will be introduced by the ground. In other words, the later the echo appears in an A-scan, the more it will be attenuated due to these two losses. To compensate for this attenuation in function of time (or depth  $R$ ), a time varying gain is introduced, giving a fixed gain in dB per unit of time (or per meter) as represented on fig 1.5. The curve would approximately compensate for a loss of 50 dB/m (spreading loss + attenuation in the ground). In practice the TVG is not an amplifier whose gain changes as a function of time, but an attenuator whose attenuation is changed as a function of time. The time varying attenuator is based on PIN diodes. PIN diodes have the property of having a variable resistance as a function of voltage and they have a low junction capacitance[21].

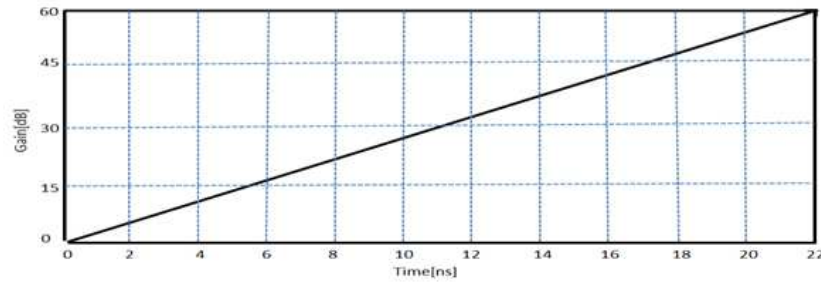


Figure 1.5: Gain curve as a function of time.

### 1.5.3 Timing circuit

The receiver in a time domain GPR is based on a non-coherent acquisition of the backscattered RF signal. This means that the acquisition must be controlled by a very stable and precise timing circuit that synchronizes the work between the different parts in the system. The timing circuit is responsible for mainly three things. First, it has to trigger the impulse generator. Secondly, the timing circuit has to generate the timing signals as needed for the sequential sampler, i.e. a trigger for the A/D converter at the intersection of the fast and the slow ramp. Third, it has to control the timing for the TVG.

## 1.6 Problems areas

GPR has many challenges like range resolution, signal processing, image processing, antenna requirements. GPR can detect the small objects under the surface, but it cannot clearly detect the complex objects. And it is difficult to GPR to distinguish mine and mine like targets. Typically GPR uses element antennas, like dipoles. They have low directivity and therefore perform best when they are in contact with the ground, to couple as much energy as possible into the ground. For safety reasons, demines do not want to use a sensor that is in direct contact with the ground.

Further, minefields have often a very rough surface and are covered with a lot of vegetation and in case of landmine detection, if antenna is in contact with the ground it slow down the speed of the GPR, it is also a problem. And another problem area is the output of a GPR is usually an image representing a vertical slice in the subsurface. These images are sometimes difficult to analyze and expert knowledge of the system and the physics behind the operating principle of the system is needed for correct interpretation of the results. Landmine like targets are very small in size and buried close to the air-ground surface. So

we need large bandwidth device to detect the landmines because the range resolution is directly related to the bandwidth.

## 1.7 Goal of the thesis

GPR can detect both metallic as well as non-metallic objects in the subsurface. GPR effectively detect the small targets that are buried close to the air-ground interface with large band width system. A larger bandwidth is needed for a better depth resolution and detailed echo. The need for larger bandwidth has led to the development of UWB GPR. The range resolution of a radar system is defined as “the ability to distinguish between two targets solely by the measurement of their ranges (distance from the radar); usually expressed in terms of the minimum distance by which two targets of equal strength at the same azimuth and elevation angles must be spaced to be separately distinguishable”. The range resolution of a GPR directly related to the bandwidth of the system (  $B$  ) and the propagation velocity  $v$  is given by:

$$\Delta R = \frac{v}{2B} \quad (1.1)$$

UWB GPR uses the ultra-wide band, ultra short pulse for transmitting into the ground. Generating UWB pulse is one of the critical functions in the UWB GPR. Goal of my thesis is generating UWB pulse with simple circuit and simple elements like transistors, resistors and capacitors.

## 1.8 Conclusion

GPR is one of the most promising technologies for detection of buried objects of various types. The range resolution of a GPR is directly related to the bandwidth of the system. The need for larger bandwidth has led to the development of UWB GPR. Generating and receiving UWB pulse is one of the most challenging area to be addressed by GPR research community to realize cost effective reliable UWB GPR system.

## Chapter 2

# UWB Pulse Generation Technology

### 2.1 Introduction

Pulsed UWB technology uses short pulses that have a very short time duration, on the order of a nanosecond or sub-nanosecond, thereby spreading the radio signal power over a wide bandwidth. This feature offers high time and range resolution, reduced multipath fading, low power and complexity, high data rates and low probability of undesired detection and interception. Pulsed UWB transceivers [8] with low-cost and low power are also preferable for wireless communication and biomedical applications such as wireless personal and sensor networks, interchip communications and UWB biotelemetry [5].

According to the FCC definition, UWB transmitter must have either :

- an absolute bandwidth  $B$  equal to or greater than 500 MHz  
i.e.  $B \geq 500MHz$

or

- a fractional bandwidth  $B_f$  equal to or greater than 0.20  
 $B_f \geq 0.20$

$$B_f = 2 \frac{f_h - f_l}{f_h + f_l} \quad (2.1)$$

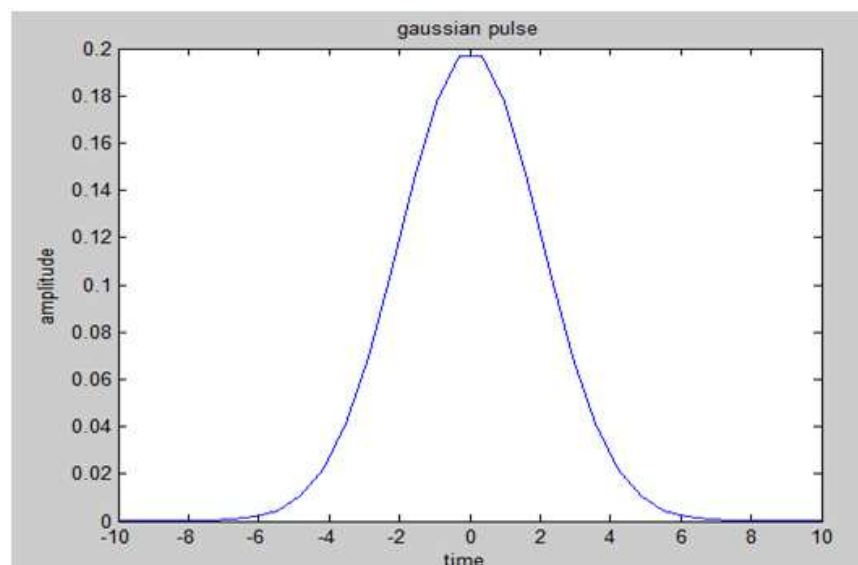


Figure 2.1: Gaussian pulse.

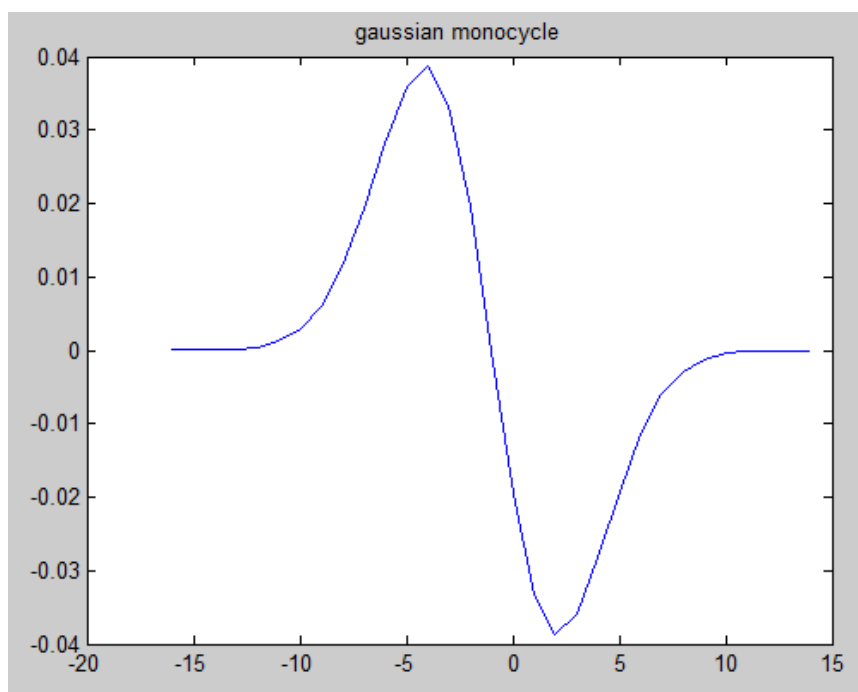


Figure 2.2: Gaussian monocycle pulse.

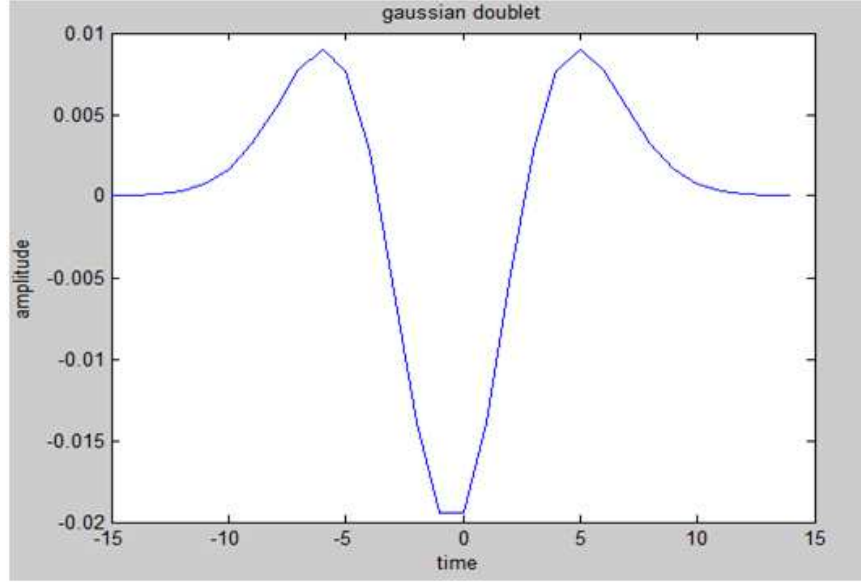


Figure 2.3: Double differentiated Gaussian pulse.

## 2.2 Types of UWB pulses popularly used in GPR

In UWB transceivers, generation of Sub-nanosecond pulses is a critical function and poses some serious challenges in circuit design. In addition to the wide signal bandwidth required, low power consumption and low complexity (for low cost) are necessary. The UWB pulse generator should be reconfigurable for different pulse shapes and spectra to provide more flexibility and to handle process variations, regulatory differences, and changes in the channel or antenna characteristics. To simplify the transceiver architecture for lower power consumption and cost, built-in modulation capability is usually desirable.

FCC is specified the frequency bandwidth and PSD for UWB devices, so there are few regulations on the characteristics of the time-domain waveform. So we have to choose the waveform that is flexible, best suits the application at hand, and the design of the UWB pulse generator can be tailored for a low hardware complexity and power consumption. In the literature it is written that Gaussian pulse and its derivatives are the most common UWB pulse shapes. The standard Gaussian pulse waveform is given by:

$$x(t) = \frac{A}{\sqrt{2\pi\sigma^2}} e^{-\left(\frac{t^2}{2\sigma^2}\right)} \quad (2.2)$$

where  $A$  is a constant amplitude, and  $\sigma$  is the original Gaussian standard deviation.

The first and second derivatives of the Gaussian pulse are widely known as the Gaussian

monocycle and doublet respectively [16]:

$$x^{(1)}(t) = -\frac{At}{\sqrt{2\pi}\sigma^3}e^{-\left(\frac{t^2}{2\sigma^2}\right)} \quad (2.3)$$

$$x^{(2)}(t) = -\frac{A}{\sqrt{2\pi}\sigma^3}\left(1 - \frac{t^2}{\sigma^2}\right)e^{-\left(\frac{t^2}{2\sigma^2}\right)} \quad (2.4)$$

The Gaussian, monocycle and doublet pulse waveforms given by equations (2.1), (2.2) and (2.3) respectively are plotted in fig 2.1,fig 2.2,fig 2.3.

## 2.3 Fundamentals of Pulse Generation Techniques

In the initial days scientists used fast step generators and microwave transmission lines to generate Gaussian-based UWB pulses. Commonly they used delay-type configuration is shown in Fig. 2.4. J.Lee used a square-wave oscillator in [13] to drive a fast-switching step recovery diode (SRD) and generate a fast-transition step signal. During the positive half-cycle of the square wave, the SRD turns on and storing some of the available charge. When the oscillator signal makes a transition into the negative half-cycle, the SRD discharges this energy and turns off abruptly, exciting the transmission lines with a fast-transition step signal. This step signal divides into two upon arriving at the junction between the main transmission line and the short-circuited stub: one propagating down the main transmission line towards the output and the other along the short-circuited stub. The pulse travelling towards the short circuit is reflected back with inverted polarity, eventually combining with the other step function to form a Gaussian impulse at the output. Here the short-circuit stub is acting as a delay line and the duration of the output pulse is thus approximately given by [13]:

$$\tau = \frac{2L_d}{v_p} \quad (2.5)$$

where  $L_d$  is the length of the short-circuit stub and  $V_p$  is the propagation velocity through it. For shorter delays and pulse durations have to use Shorter stubs. But excessive reduction of the stub length could reduce the pulse amplitude significantly, as the delay becomes too short compared to the rise time. This pulse generator can produce pulses with 154 ps time duration, 3.5 V amplitude and good shape symmetry With a pulse repetition frequency (PRF) of 10 MHz[13].

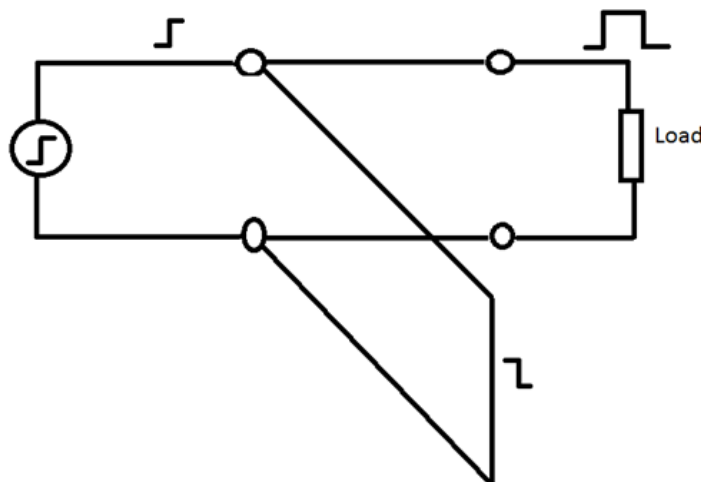


Figure 2.4: Gaussian pulse generator using a fast step generator and transmission lines.

### 2.3.1 Transmission line based Pulse Generators

In [10, 24] The impulse duration is tuned by varying the length of the short-circuited stub Ld. In [10], by using diodes or MESFETs connected to ground at multiple Locations loaded the transmission line thereby synthesizing a short-circuited stub with a variable length. The pulse time duration and amplitude varies from 300 ps to 800 ps and 1.3 V to 1.9 V respectively using MESFETs [10]. In [24], main transmission line is connected to one of multiple short-circuited stubs with different lengths by using diodes, allowing the pulse duration to vary from 300 ps to 1 ns.

This concept was extended in [5] to generate the monocycle pulse from the Gaussian pulse. In [12, 14, 24] the monocycle pulse is generated by using a second short circuited stub to combine two of the generated Gaussian pulses with opposite polarities and a time delay between them. The duration of the produced monocycle is about twice that of each individual Gaussian pulse. In [5], the monocycle pulse is generated directly by differentiating the Gaussian pulse using an RC high-pass filter. Therefore the resulting pulse duration can be reduced to be almost the same as that of the Gaussian pulse before differentiation. In [5], the fabricated microstrip circuit generates a monocycle pulse with 300ps time duration, 200mV peak-to-peak voltage, -17dB ringing level, and good pulse symmetry.

Although these all pulse generators can provide ultra-short Gaussian-based pulses exhibiting high voltage amplitude and good symmetrical shape, they inherently employ some specific components such as SRDs, making them quite difficult to integrate with standard digital



CMOS circuits.

### By using Schottky Diode

In [9] Jeongwoo Han and Cam Nguyen introduced new ultra-wideband (UWB), ultra-short, step recovery diode monocycle pulse generator. This pulse generator uses a simple RC high-pass filter as a differentiator to generate the monocycle pulse directly.

The pulse-shaping network employs a resistive circuit to achieve UWB matching and substantial removal of the pulse ringing, and rectifying and switching diodes to further suppress the ringing in fig 2.5 showing the schematic of the new monocycle pulse generator. It consists of three parts: Gaussian pulse generator, pulse shaping network, and RC network.

This Gaussian pulse generator produces a Gaussian pulse in two distinct steps. First, SRD creates a step function with short transition time and it passes through the main transmission line and short circuit stub, the one it is passing through the short circuit stub reflect back with opposite polarity. Second, an impulse is formed by combining the step function reflected from the short-circuited stub and that transmitted across the junction between the short-circuited stub and the transmission line. The duration of the Gaussian pulse is Depends on the length of the short-circuited stub.

The pulse-shaping network consists of a series-connected Schottky diode, a terminated shunt stub, a blocking capacitor, and a shunt Schottky diode with biasing circuit. The main function of the pulse shaping network is, It provides wide-band impedance matching between the Gaussian pulse generator and the RC network, and it is preventing the Gaussian pulse from having a large ringing level and effectively shaping the pulse waveform. The circuit gives a very large ringing results when the pulse-shaping network is not used. This is due to the severe impedance mismatch between the Gaussian pulse generator and RC network. The Gaussian pulse and its ringing occur over an ultra-wide bandwidth, so we need a lossy matching network. This lossy network attenuates the pulse amplitude. Here the diode acts as a half-wave rectifier, passing only the positive parts (Gaussian pulse and positive ringing) and removing the negative ringing portion. This diode functions as a fast switch only allowing passage of parts of the signal whose amplitudes are greater than a threshold voltage controlled by the dc bias voltage. When compare to the amplitude of the Gaussian Pulse, the ringing level arriving at the Schottky diode is very small , it can be removed by setting a small threshold level thereby not sacrificing the pulse amplitude. Gaussian waveform is shifted down by the dc bias voltage. This voltage offset, however, cannot pass through the capacitor in the following RC network and thus, will not be seen in the monocycle pulse.

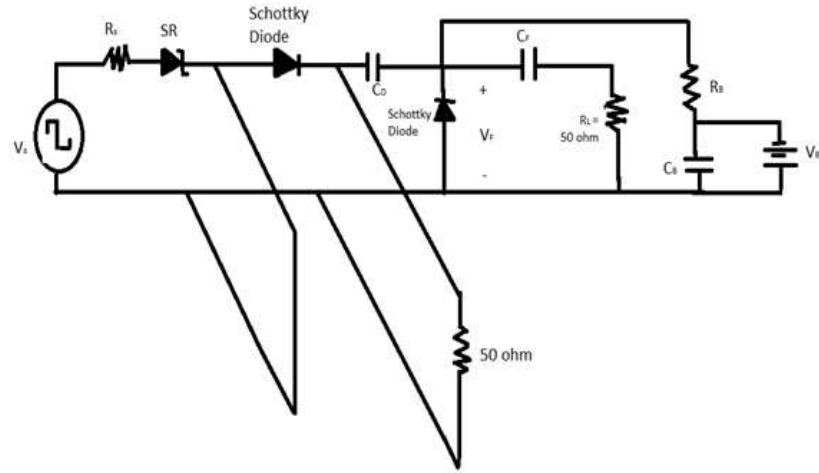


Figure 2.5: Schematic of the new monocycle pulse generator.

The RC network consists of a capacitor and a load resistor. The capacitance is determined by the load resistance and required time constant. This time constant can be estimated from the Gaussian pulse duration and the settling time of the exponentially decay response of a step function to the RC network. Here they fabricated the new monocycle pulse generator using microstrip line on FR-4 glass epoxy substrate having a relative dielectric constant of 4.5 and a thickness of 0.031 in. The fabricated microstrip monocycle pulse generator produces an ultra-short monocycle pulse with 300-ps pulse duration, -17dB ringing level, and good pulse symmetry. Because of the simplicity, low cost, and good performance of this circuit makes it attractive for various UWB radar and communications systems.

### By using attenuator and transmission lines

In [20] Alexandre SERRES, Yvan DUROC introduced a new simple Ultra-Wideband (UWB) monocycle pulse generator based on step recovery diode. This pulse generator uses nonlinear components with a single power supply and microstrip transmission lines. It has the three main parts: a Gaussian pulse generator, an impulse-shaping network, and a monocycle-pulse forming circuit.

The first part of the circuit is an analog Gaussian pulse generator. It is shown in fig 2.6. It uses a step recovery diode (SRD) which is the most common used source to generate UWB pulses. The main work of a SRD is to work as a charge controlled switch using a P-I-N junction with faster switching characteristics than a typical PN junction. A stored charge is created in the junction as a result of the minority carriers inserted during the forward bias

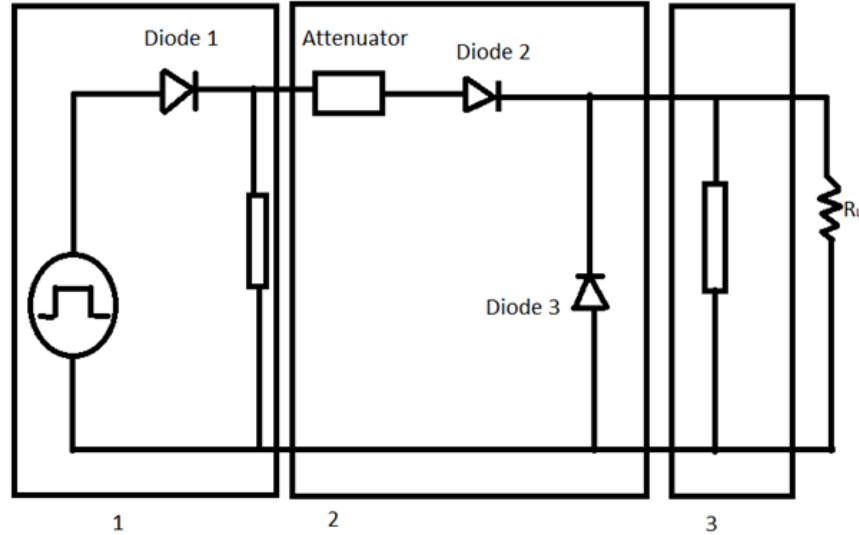


Figure 2.6: Circuit of the monocycle-pulse generator.

state, where a recombination time (or carrier lifetime) must occur. The junction impedance is abruptly dependent on the stored charge, which has the capability to lead to fast rise time pulses. In any case diode appears to have a low impedance until the charge within the junction is depleted. Then, the diode snaps back into a high impedance state, essentially stopping the reverse current of the SRD. This impedance transition, along with the current within the SRD prior to cutoff, causes a voltage spike [3]. The amount of time for this transition is called as "snap" time, and because of this we call SRD as snap diodes. The typical snap time ranges vary from 30 to 250-ps, allowing SRD to generate pulse widths on the order of picoseconds.

One common SRD Gaussian pulse generator configuration is shown in fig 2.7. Here the SRD is driven by an external 100-MHz oscillator. The ramp-like pulse produced by the SRD splits at point A, traveling down the reverse transmission line and also propagating down the forward transmission line. The ramp like pulse moving towards the reverse transmission line reflects back because of the stub. Then, it is converted into an opposite polarity ramp-like time delayed pulse due to the negative reflection coefficient of the short circuit. At the forward transmission line, the two pulses recombine to form a Gaussian pulse shape. The width of the pulse is depends on the length of the short circuited transmission line. The obtained Gaussian pulse shape is distorted and more ringing occurred due to the fast rise time of the pulse. Here a negative voltage appears before the pulse due to the carrier lifetime of the SRD. The pulse shaping network remove this negative voltage. The second

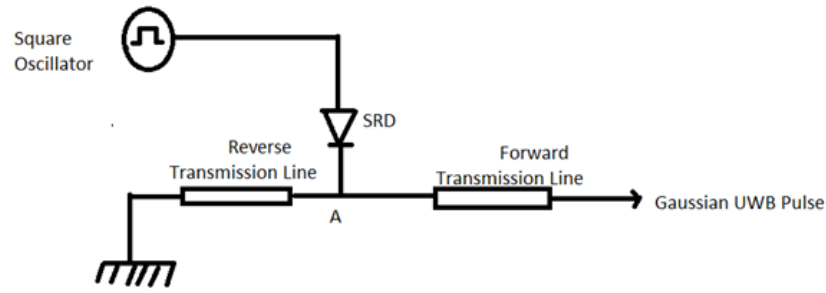


Figure 2.7: Schematic of a SRD pulse generator.

part of the figure.1 is pulse shaping network.

It has the series Schottky diode (Diode 2) removes any negative ringing, essentially acting as a half-wave rectifier. Any voltage below the forward voltage of approximately 0.6-volts in the input waveform causes the diode to be reversed biased, which effectively disables the output until the input reaches a positive voltage state. The shunt Schottky diode (Diode 3 in fig 2.6) reduces the ringing in the pulse train by acting as a switch. When the pulse passes through the shunt diode section, the current is switched off due to the surge in voltage, allowing the pulse to pass through without distortion. Once the voltage surge subsides, the diode switches back on, which enables it to become a short circuit again. Here the ringing acts as an AC waveform and its voltage is not enough to reverse bias the diode, so it passes through the diode to ground due to the low impedance.

The third part of the fig 2.6 is monocycle-pulse forming circuit. It converts the Gaussian pulse in a Gaussian monocycle using a short-circuited transmission line. The shaping network splits the impulse into two impulses arriving at the junction of the transmission line and the output of the circuit. The impulse propagating toward the short circuit is reflected back and combined with the other impulse transmitted. This generator produces 270-ps monocycle pulses with about a 1.7-V peak to peak amplitude.

### By using Latches

In [17] Reisenzahn A, introduced A new low-cost pulse based ultra-wideband radar system working up to 6.4 GHz. Pulse generated with a simple transistor circuitry. Here the authors goal is an easy way to manufacture UWB-pulse generator with off the shelf parts possibly without biasing of parts with varying parameters. Here they used the step recovery effect of bipolar transistors to generate the steep edged pulses.

The transistor is driven into saturation where both junctions, base-collector and base-emitter

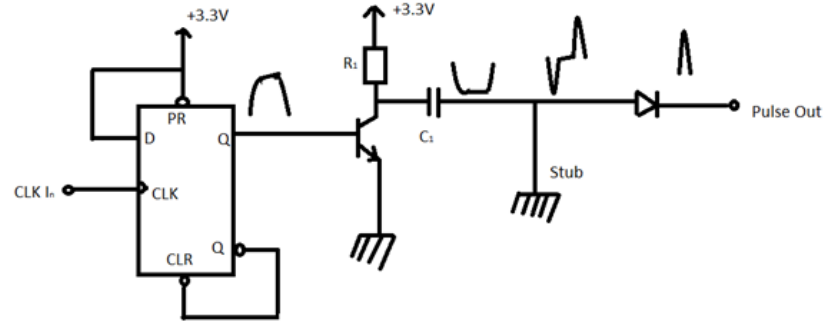


Figure 2.8: Schematic of the pulse generation circuit.

junctions get forward biased. If the transistor is reverse biased the base-collector junction will remain in low impedance state until the earlier in the junction stored minority carriers are removed completely. The result is an abrupt change to high impedance which causes the collector current to turn to zero immediately. A steep rising edge is generated at the collector of the transistor. A schematic of the proposed circuitry is depicted in Fig 2.8.

Here to switch the transistor a D-latch was used. This generates a 2.5 ns long pulse with an amplitude of about 2.3 V at a 50 ohm load used to drive the transistor into saturation. The only additional parts are the resistor  $R_1$  between the supply voltage and the collector and the capacitor  $C_1$  for DC decoupling.

Here the negative output pulse has a much steeper rising edge caused by the step recovery effect. But the pulse length is quite the same. The signal is differentiated with a high pass filter to generate shorter pulses, it results two short pulses – one negative and one positive. Here the filtering was realized with a short circuited stub. The impedance of the stub line should be as high as possible to have less influence on the pulse at the line. Then it passes through the diode, the diode allows only the positive pulse and it rejects the negative pulse. Finally it generates a Gaussian pulse. The output of this generator giving a rectified nearly Gauss-shaped pulse with a duration of 100 ps and an amplitude of 0.57 V.

### 2.3.2 CMOS based UWB Pulse Generators

Recently many alternative UWB pulse generators proposed in the literature, which are integrated into digital CMOS for a low cost and also provide reconfigurable pulse shapes and frequency spectra. CMOS chip can provide the good power levels with a fast rise time

for short-range UWB applications. Four main new techniques proposed here are carrier-based, analog filtering, digital filtering and direct digital synthesis.

### Carrier-based Approaches

Heterodyning and time-gated oscillators are used in Carrier-based UWB pulse generation techniques. In heterodyning, a pulse is first generated at baseband with a low-pass spectrum and then upconverted to the target frequency band. This typically employs a local oscillator (LO) and a mixer (multiplier) with the architecture shown in Fig.2.9

Control of the radiated center frequency is achieved by the LO, which can either have a known fixed frequency or be voltage-controlled for frequency-hopping and multiband applications. By manipulating the time duration of the baseband pulse, we can control the radiated bandwidth. As shown in Fig. 2.9, frequency up conversion can relax the signal bandwidth required from the baseband pulse generator. Another variant of this is derived through the use of time gating as illustrated in Fig. 2.10, where the output of a continuously-running LO is time gated using an external switch, and/or the LO itself is switched on and off. The output generated by this approach typically exhibits a few cycles of the LO having a rectangular amplitude envelope, which can result in an inefficient sinc spectrum with high out-of-band power that will need to be filtered [5].

Recently Cavallaro et al. [16,19] demonstrated an UWB pulse generator based on the heterodyning technique in 90 nm CMOS. The Local Oscillator is designed by using an inductor-capacitor (LC) voltage-controlled oscillator (VCO) locked in a phase locked loop (PLL). A switched capacitor bank is added in the LC VCO to synthesize carrier frequencies between 3.5 GHz to 4.5 GHz in steps of 500 MHz. The carrier is then BPSK modulated using Gilbert cell. To reduce LO leakage between pulses, A switch is added at the output of the BPSK modulator. A ramp generator and a pseudo-Gaussian envelope generator (PEG) form the baseband pulse generator in this design. To produce a staircase waveform the ramp generator uses a shift register and a digital-to-analog converter (DAC) and it is smoothed by a low pass filter. The PEG then creates a Gaussian like baseband pulse using the ramp signal as the input. It mainly consists of two differential pairs with their outputs cross-coupled to each other.

An offset is introduced between the gate overdrive voltages of the two differential pairs, causing the net output current of the cross-coupled structure to rise and fall for a Gaussian like current impulse. Pseudo-Gaussian pulse is generated and it is upconverted to the LO

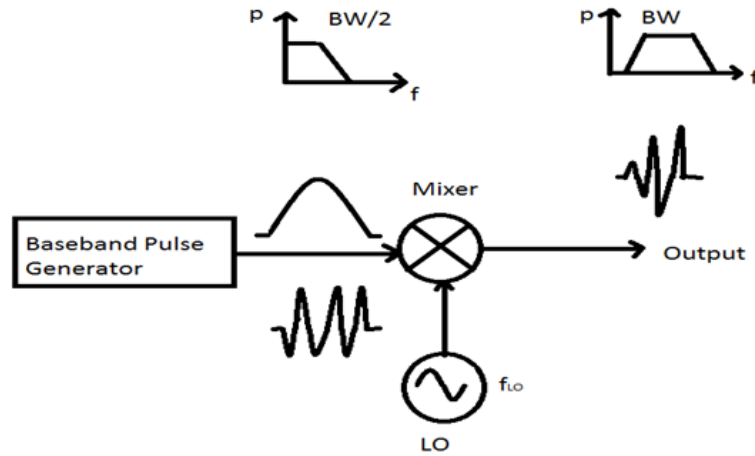


Figure 2.9: Heterodyning for pulse generation.

frequency band using a folded Gilbert quad. Measurements were demonstrated showing 4 GHz pulses with a Gaussian amplitude envelope. The pulse peak-to-peak voltage is 200 mV and the LO ringing level is below 3 mV. The pulse time duration is 2.8 ns for a 628 MHz -3 dB bandwidth. The maximum PRF can reach 500 MHz and the energy dissipated per pulse is 56 pJ. Switched local oscillators have also been investigated for UWB pulse generation. In [16], to generate an UWB pulse an LC oscillator is switched on and off in response to the digital data. A switched capacitor bank is used in the LC oscillator to be able to switch the oscillation frequency to one of three 528 MHz sub bands centered at 3.5 GHz, 4 GHz and 4.5 GHz. A triangular pulse envelope is realized by exploiting the turn-on and turn-off transients of the LC oscillator. By simply activating the tail current source the oscillator is turned on. The rise time, which is designed to be one half of the pulse duration for a symmetrical triangular pulse shape, should be in the range of 1 ns for more than 500 MHz of bandwidth. It can be reduced by increasing the transconductance of the active devices, which typically requires increasing the DC current. Depending on power consumption and technology achieving a rise time on the order of a nanosecond is a challenging thing. The oscillator turn off procedure involves simultaneously switching off the tail current source and activating an NMOS switch across the LC tank. The equivalent parallel resistance across the LC tank for a shorter turn off transient is reduced by on-resistance of the switch. The size and on-resistance of the NMOS switch is designed to make the fall time equal to the rise time for a symmetrical triangular pulse. The circuit was fabricated in  $0.18\mu\text{m}$  CMOS with a die area of  $560\mu\text{m} \times 550\mu\text{m}$ . Measurements were demonstrated showing an output pulse with a peak-to-peak voltage of 160 mV, a time duration of 3.5 ns and a 520 MHz

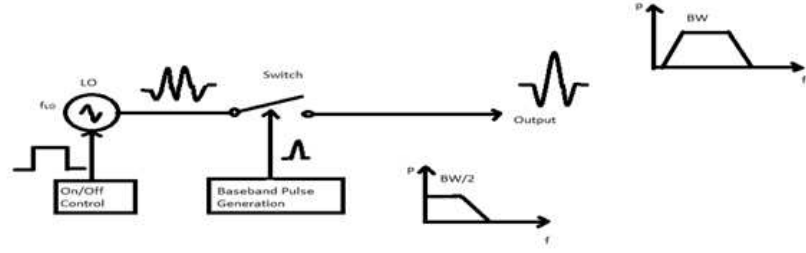


Figure 2.10: Alternative time gating for pulse generation.

bandwidth at 100 MHz PRF. The energy dissipated per pulse is only 16.8 pJ [5].

Sim et al. [16] presented a pulse generator for 6-10 GHz UWB applications based on the switched oscillator technique. A pulsed three-stage ring oscillator followed by an on-chip pulse shaping filter is proposed. The oscillation frequency of the oscillator have in the center of the 6 - 10 GHz band around 8 GHz. To generate an UWB pulse with a rectangular amplitude envelope, it is quickly switched on and off over a short time duration. Due to the low quality factor ( $Q$ ), the ring oscillator has a fast on/off transient response. A high-pass LC filter is used to suppress the out-of-band spectral components. The circuit was fabricated in 0.18 CMOS, occupying an area of 0.11 mm<sup>2</sup>. The average power consumption is 1.38 mW at a supply voltage of 2.1 V for a PRF of 50 MHz. This corresponds to a low energy consumption of 27.6 pJ per pulse. Time- and frequency-domain measurements showing that pulse peak-to-peak amplitude of 673 mV, a pulse time duration of 500 ps and a -10 dB bandwidth of 4.5 GHz from 5.9 to 10.4 GHz.

### Analog Filtering

A common way to generate an UWB pulse directly without using a carrier is to form a baseband impulse first with a very short time duration and a high frequency bandwidth, and then filter the impulse using a bandpass or a pulse shaping filter as illustrated in Fig. 2.11. This type of designs is typically more suitable for non frequency agile applications, as the UWB signal's center frequency and bandwidth are primarily determined by the bandpass or pulse shaping filter.

In [5] Zheng et al. proposed a CMOS circuit that directly performing the squaring, exponential and second derivative functions required to generates the Gaussian doublet.



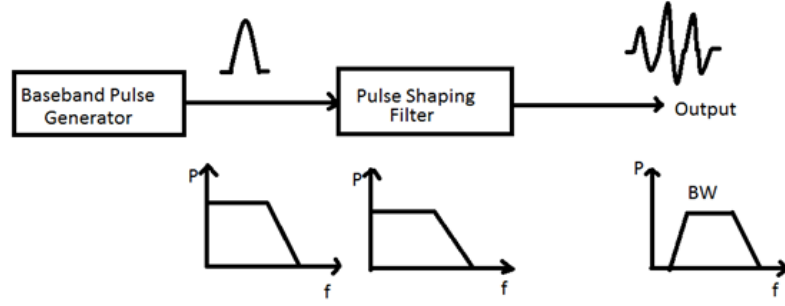


Figure 2.11: Filtering for pulse generation.

For the squaring circuit, a transistor operating in the saturation region is used. To reduce velocity saturation and channel length modulation effects [5] non-minimum channel length is chosen for this transistor. Exponential circuit consisted of a transistor biased in the subthreshold or weak inversion region. In the absence of a conducting channel the n+source, p bulk and n+ drain form a parasitic bipolar transistor. In this region current-voltage relationship is exponential and can be approximated

$$I_{DS} = I_{DO} \exp\left(\frac{V_{GS}}{\lambda}\right) \quad (2.6)$$

where  $I_{D0}$  and  $\lambda$  are CMOS process dependent parameters. Finally, an LC network second-order differentiator (Fig. 2.12) is used at the output. The transimpedance VO can be expressed in the frequency domain (s-domain) as:

$$\frac{V_{out}(S)}{V_{in}(S)} = \frac{-sR_L L}{R_L + sL + \frac{1}{sC}} \approx -s^2 R_L L C \quad (2.7)$$

Where the approximation is valid if the value of inductor L and capacitor C satisfy the  $R_L + sL \ll \frac{1}{sC}$ . This is readily achieved in the UWB frequency range with the typical values of on-chip spiral inductors and MIM capacitors. The circuit was fabricated in  $0.18\mu m$  CMOS and tested with a 200 MHz input clock . The output voltage is a second-order

derivative of the current  $I_{IN}$ . The measured output pulse has a Gaussian doublet shape and a good symmetry. It has the time width of less than 0.8 ns and a -10 dB bandwidth of approximately 2 GHz in the 3 GHz to 5 GHz band. The maximum peak-to-peak amplitude is limited to about 35 mV, giving rise to the need for subsequent wideband amplification. This is because of the low sub threshold current levels in the exponential circuit and the significant insertion loss of the differentiating LC network.

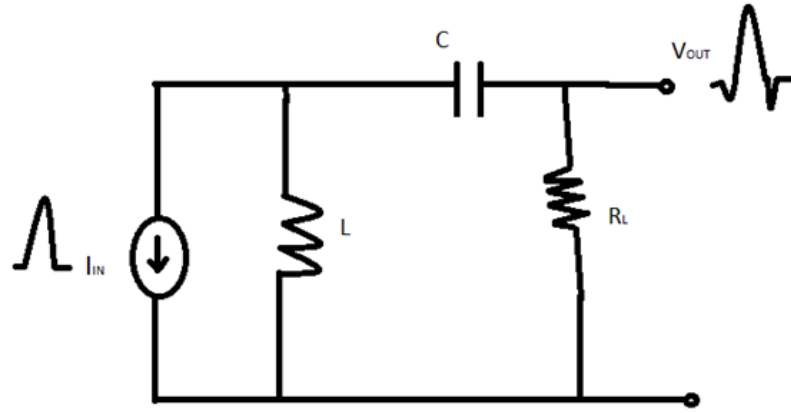


Figure 2.12: RLC pulse shaping circuit as a second-order differentiator.

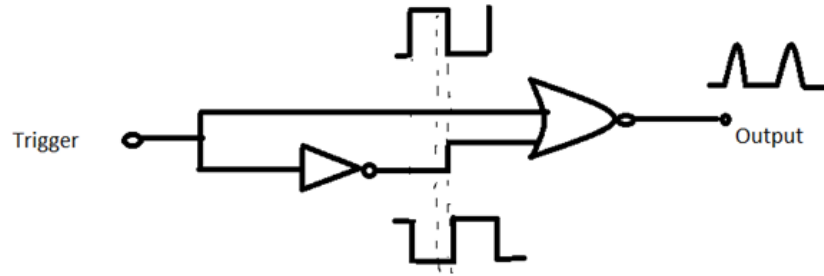


Figure 2.13: Digital logic for impulse generator.

In [5] S. Bourdel et al. demonstrated a pulse generator using digital logic for baseband impulse generation and a third order LC ladder Bessel filter for UWB pulse shaping. Digital logic circuits gives the baseband impulses as shown in Fig 2.13. They are having inverters to introduce a small delay followed by a NOR gate to generate an impulse on every falling edge of a trigger signal. The relative timing of the signals at the input of the NOR gate is shown in Fig 2.13. The NOR gate combines the falling edge of the trigger signal and its delayed inverted replica to form a positive impulse. We can use NAND gates also in place of NOR gates to realize impulses with the opposite polarity on every rising edge of the trigger. They used high-speed current mode logic (CML) for the delay cell to create a baseband impulse with a very short time duration of 75ps and a at frequency spectrum out to 10 GHz. The

generated impulse is then applied to the third-order LC ladder Bessel filter to form the UWB pulse. To limit its signal power loss to within 3 dB, the filter order is kept to three which arises due to the low quality factor (Q) of on-chip passive devices. The measured pulse peak-to-peak amplitude and time duration are 1.42V and 460 ps respectively. The IC occupies an area of  $0.54 \text{ mm}^2$  in  $0.13\mu\text{m}$  CMOS technology and consumes 3.84 mW of power at 100 MHz PRF.

In [5] Kawano et al. designed a pulse generator in  $0.13\mu\text{m}$  Indium Phosphide (InP) technology for 22-29 GHz UWB applications using a filter-based technique. By using baseband impulse with a peak-to-peak voltage of 0.8 V, a very short time duration of only 9 ps is first generated that has a frequency spectrum in the 22-29 GHz band. The baseband pulse generator is similar to that of Fig 2.8 and consists of a CML delay inverter and a CML AND gate. Here cascade circuit configuration is used in the AND gate to reduce the miller capacitance and increase the switching speed for an ultra-short impulse. The chip area and power consumption of the baseband pulse generator is  $1.5 \text{ mm} \times 1.7 \text{ mm}$  and 620 mW respectively. For pulse shaping a cosine roll-off bandpass filter (BPF) is used with a roll-off factor between 0.9 and 1 to reduce the ringing level at the cost of a longer pulse duration. Because of the low quality factor (Q) of on-chip inductors and capacitors at millimeter wave frequencies, Transmission lines are used to realize the BPF. The measured insertion loss of the BPF is 2.6 dB at the center frequency of 26.5 GHz, and the attenuation is about 16 dB and 26 dB at 24 GHz and 29 GHz respectively. The chip area of the BPF is  $8 \text{ mm} \times 5 \text{ mm}$ . The generated UWB pulse has a time duration of less than 500 ps and ringing level of less than -20 dB and swing of about 60 mV.

### Digital Filtering

An alternative to analog filtering is a technique based on a digital filter as shown in Fig. 2.14. Multiple delayed copies of a baseband impulse can be individually scaled with the desired polarity and amplitude, and then added together to form an UWB pulse.

By using this method, we can more control the UWB pulse waveform and frequency spectrum. Here a trigger signal is distributed to N baseband pulse generators (BPG) using a digital delay line, with a time delay of  $T_D$  per stage. This triggers the BPGs to produce impulses at sampling times of  $T_D, 2T_D, \dots, NT_D$  with a sampling frequency of  $f_s = \frac{1}{T_D}$ . Then these signals are scaled with tap coefficients  $c_i$ ,  $i = 1; 2; \dots; N$  using amplifiers. The resulting pulses are finally combined by a wide band pulse combiner at the output. From this method, another method is derived i.e by directly scaling the delayed edges of the trigger

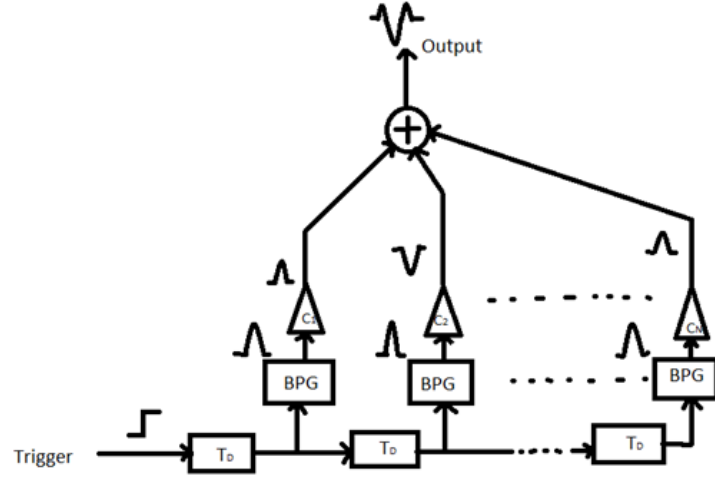


Figure 2.14: Baseband impulse combination for UWB pulse generation.

signal and combining them, without generating baseband impulses as shown in Fig. 2.15. Here the sum of all of the tap coefficients  $c_i$   $i = 1; 2; \dots; N$  must be equal to zero, to ensure that the generated pulse has a finite time duration.

### Direct Digital Synthesis

Another approach for UWB pulse generation is waveform synthesis based on highspeed digital-to-analog converters (DAC) as shown in Fig. 2.16. In this a high speed DAC is used with a good resolution to generate directly UWB pulses with different shapes and it is fully reconfigurable. This type of DAC-based UWB pulse generator requires a sampling rate of more than the Nyquist rate, e.g., more than 20 GHz for a 3- 10 GHz UWB pulse.

In [5] they used a 20 GHz 6-bit DAC for UWB pulse generation, creating various pulse shapes and supporting several modulation formats. The high sampling rate poses a real challenge not only for the DAC, but also for generating the input digital data stream. This technique leads to power-hungry high speed digital CML circuits, using more advanced technologies such as SiGeBiCMOS [17]. Therefore, it is giving a command to influence some analog and RF techniques to reduce the required power consumption in an UWB pulse generator.

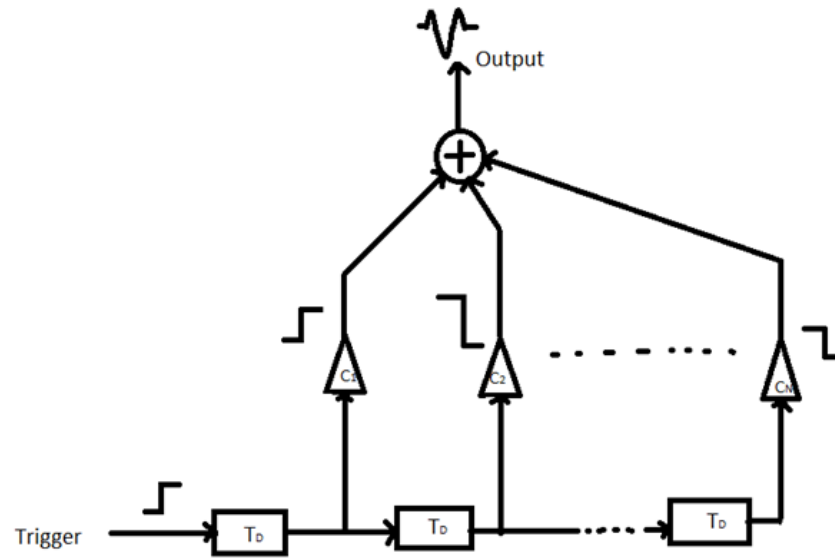


Figure 2.15: Trigger edge combination for UWB pulse generation.

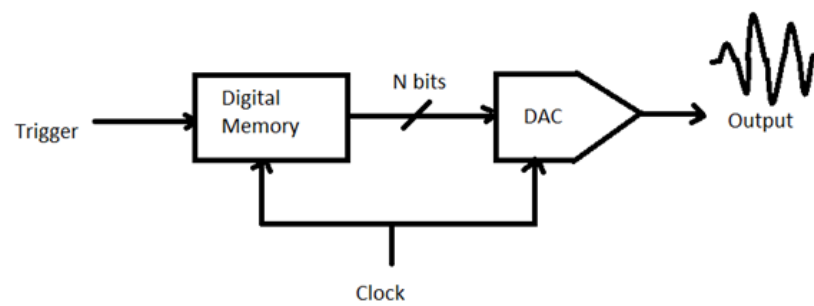


Figure 2.16: Direct digital waveform synthesis for UWB pulse generation.

## 2.4 Methods to approach:

Because of the limitation of the instruments and devices, we chosen UWB pulse generators based on transistors. In this project we have chosen two transistor UWB pulse generators. First one is based on normal transistors, and the second one based on avalanche transistor.

### Transistor based UWB pulse generator:

The circuit provides the Gaussian pulse when activated by a square wave. This pulse generator uses a simple common emitter amplifier followed by RC high-pass filter. In this circuit we can tune the pulse width duration by varying the slope of the square wave.

Figure 2.18 showing that, V1 and V2 voltage level must be in opposite phase. The two transistors in this way are respectively in an off and on state. By supposing that transistor TR1 is in “off” state and TR2 in “on” state, so V1 and V2 are respectively low and high, the same transistors driven by the linear, and opposite in phase, edge of the applied square wave signal, generate a Gaussian pulse. The advantage of this generator is low-complexity, low cost, and versatile, so we can use this generator in a variety of integrated circuits UWB modulation schemes and systems.

### Avalanche transistor based UWB pulse generator:

Fig 2.19 is a basic circuit of avalanche transistor. The static load resistance of avalanche transistor is RC. Before trigger pulse coming, the base is zero bias and the avalanche transistor works in cutoff region. According to Figure 3.6 a set of circuit equations can be listed.

$$\begin{aligned} i &= i_R + i_A \\ U_{CE} &= E_C - i_R R_c \\ U_{CE} &= u_c(0) - \frac{1}{C} \int_0^{t_A} i_A dt - i_A R_L \end{aligned} \tag{2.8}$$

In (2.10),  $i$  is the total current,  $i_R$  is the current of static load  $R_C$ ,  $i_A$  avalanche current,  $u_c(0)$  the initial voltage of capacitor C,  $R_L$  the dynamic load resistor,  $R_c$  static load resistor, C avalanche capacitor,  $t_A$  avalanche time. Solving (1), obtain the equation of dynamic load line in the course of avalanche. The avalanche transistor has regularly four working regions: saturation region, linearity region, cutoff region and avalanche region. When high enough negative voltage is loaded on collector-emitter, a strong electric field is produced in collector

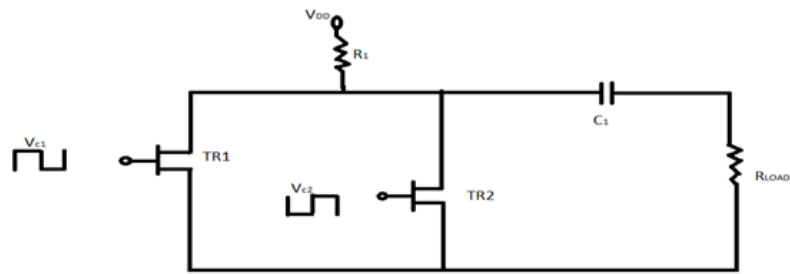


Figure 2.17: BJT based Pulse generator architecture.

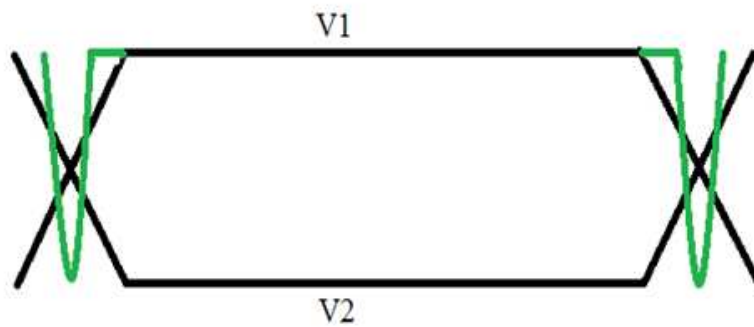


Figure 2.18: Control Signals and generated Gaussian pulse.

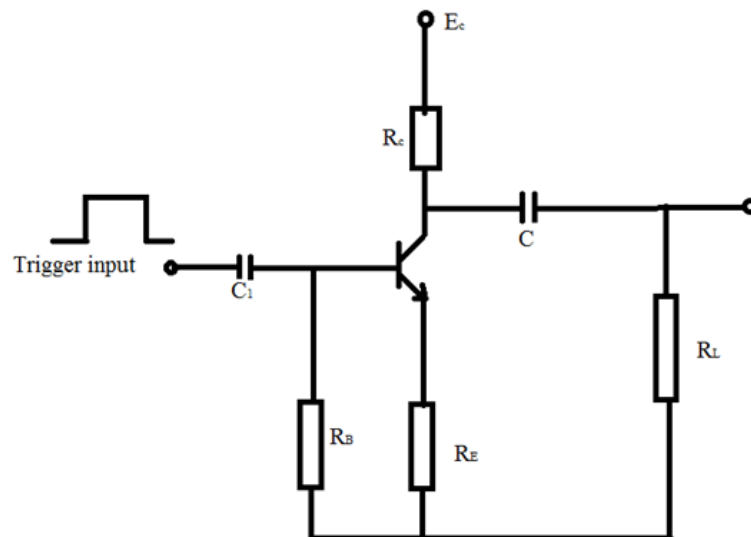


Figure 2.19: Avalanche transistor UWB pulse generator.

junction. Then the strong electric field will accelerate minority carriers which go into this space to crash into lattices in this space, so that electron-hole pairs come into being. The new electron-hole pairs are again accelerated to produce more electron-hole pairs, so the collector current runs up just like “avalanche”, which is called avalanche effect.

## 2.5 Summary and Conclusion:

In this chapter we discussed about different techniques to generate UWB pulse, and we classified the pulse generation techniques into two, one is Transmission line based Pulse Generators, and the second one is CMOS based UWB Pulse Generators. Under the Transmission line based Pulse Generators, we discussed about three techniques, the first one is using Schottky diode, the second one is using attenuator and the third one is using latches. Under the CMOS based UWB Pulse Generators, we discussed four techniques, the first one is using carrier, second one is using analog filtering, third one is using digital filtering and the fourth one is using direct digital synthesis. Because of the limitation of the instruments and devices, we chosen UWB pulse generators based on transistors. In this project we have chosen two transistor UWB pulse generators. First one is based on normal transistors, and the second one based on avalanche transistor.



## Chapter 3

# IMPLEMENTATION OF THE PULSE GENERATOR CIRCUITS

### 3.1 Introduction

In this work, we implemented two low-complexity, low cost UWB pulse generator circuits. The first one is by using the normal transistor 2N2222A, this circuit gives the Gaussian pulse when activated by a square wave input. This pulse generator uses a simple common emitter amplifier followed by RC high-pass filter. In this circuit we can tune the pulse width duration by varying the slope of the square wave. The second one is by using the avalanche transistor. This pulse generator also uses a simple common emitter amplifier followed by RC high-pass filter. This circuit also provides the Gaussian pulse when activated by a square wave input.

### 3.2 Transistor based UWB pulse generator

This pulse generator uses a simple common emitter amplifier followed by RC high-pass filter to generate UWB pulse. Here in this circuit we used 2N2222A transistor in place of TR1 and TR2. And we used R1 is 10 kilo ohm, C1 is 0.47  $\mu$ F and RLOAD is 1 kilo ohm. And here we used dc power supply i.e. VDD is 3.3Volts. and we simulated the circuit by using the MULTISIM 11.0 tool. The simulated circuit is shown in figure 3.1

We simulated the circuit. Here we used 3 kHz square wave input with 5 volts peak to peak voltage in place of V1 and V2, but with opposite polarity, and we got the Gaussian pulse

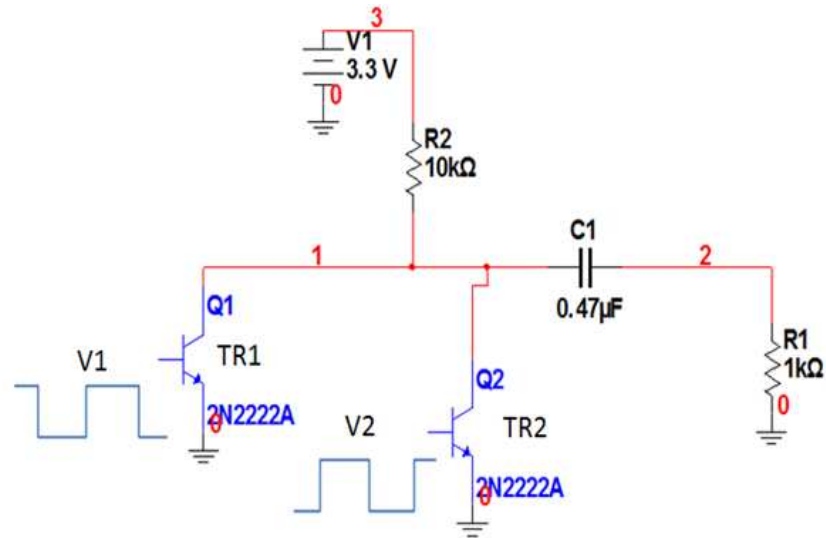


Figure 3.1: Gaussian Pulse Generator and Control Signals.

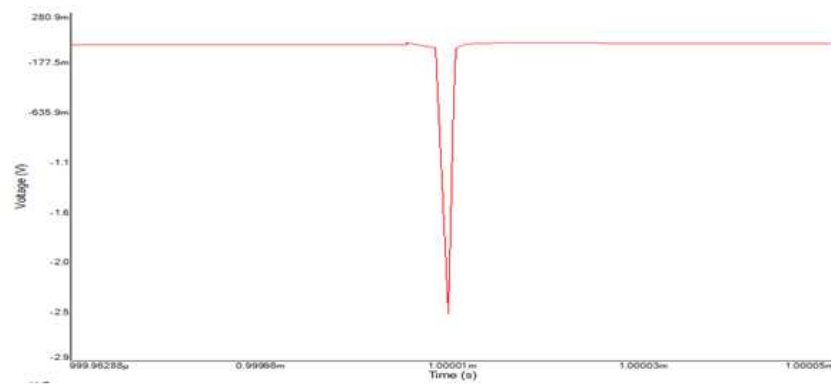


Figure 3.2: Simulated Result.

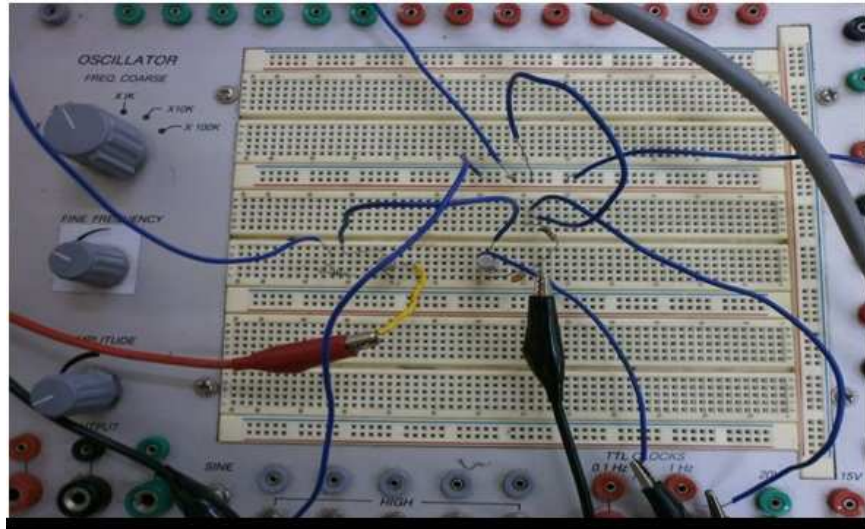


Figure 3.3: Photo of the Implemented UWB Gaussian pulse generator on Breadboard.

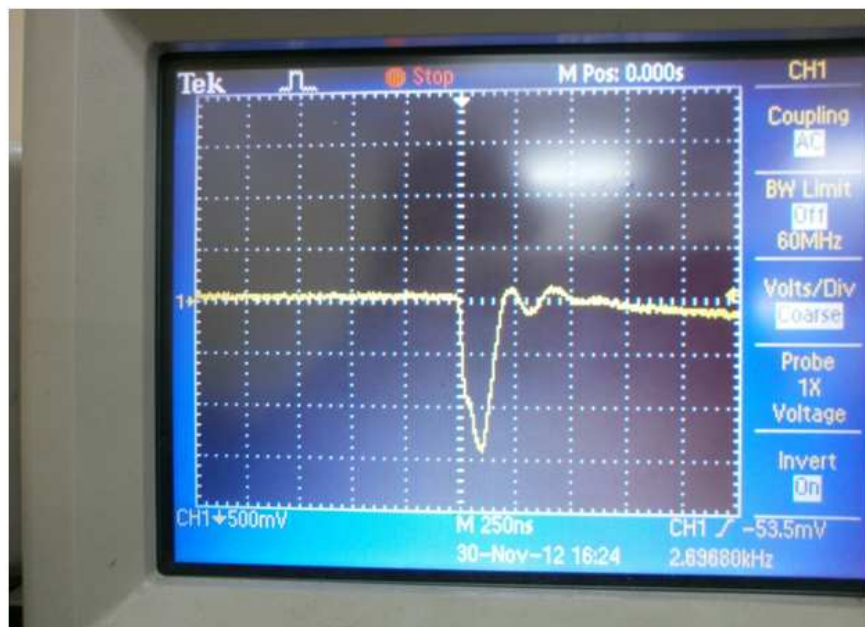


Figure 3.4: Photo of the OUTPUT of the Implemented UWB Gaussian Pulse Generator.

Parameter	Simulated	Practical
Amplitude	-2.8V	-1.45V
Rise Time	55ns	85ns
Pulse Width	173ns	200ns

Table 3.1: Summary of BJT Based UWB pulse generator circuit

output. Then we implemented the same circuit with same values on the breadboard, and we achieved the Gaussian pulse practically. In simulation we got 173ns duration Gaussian pulse, but in practical implementation we got 200ns duration Gaussian pulse.

### 3.2.1 Conclusion

In this work we presented a low complexity and low cost tunable pulse generator architecture suitable for UWB GPR applications. The circuit provides a Gaussian pulse when activated by a square wave edge of an external trigger signal from signal generator, also the pulse width duration tenability by varying the frequency. Here we used 3 kHz square wave and get 200ns duration Gaussian pulse, by increasing the frequency of the square wave, can get very short duration Gaussian pulse. Here we demonstrated the Gaussian pulse generation with reduced ringing levels, and good symmetry.

## 3.3 Avalanche transistor based UWB pulse generator

This pulse generator uses a simple common emitter amplifier followed by RC high-pass filter to generate UWB pulse. Here we used 2N5551 avalanche transistor to generate UWB Gaussian pulse. And we used  $R_{cc}$  is 10 kilo ohm,  $C_{cc}$  is 0.47  $\mu$ F,  $R_{BE}$  is 1 kilo ohm,  $R_E$  is 1 kilo ohm and  $R_L$  is 100 ohm. And here we used dc power supply i.e.  $V_{cc}$  is 12Volts. and we simulated the circuit by using the MULTISIM 11.0 tool. The simulated circuit is shown in figure 3.5.

We simulated the circuit. Here we used 3 kHz square wave input with 10 volts peak to peak voltage, and we got the Gaussian pulse output. Then we implemented the same circuit with same values on the breadboard, and we achieved the Gaussian pulse practically. In simulation we got 2 ns duration Gaussian pulse, but in practical implementation we got

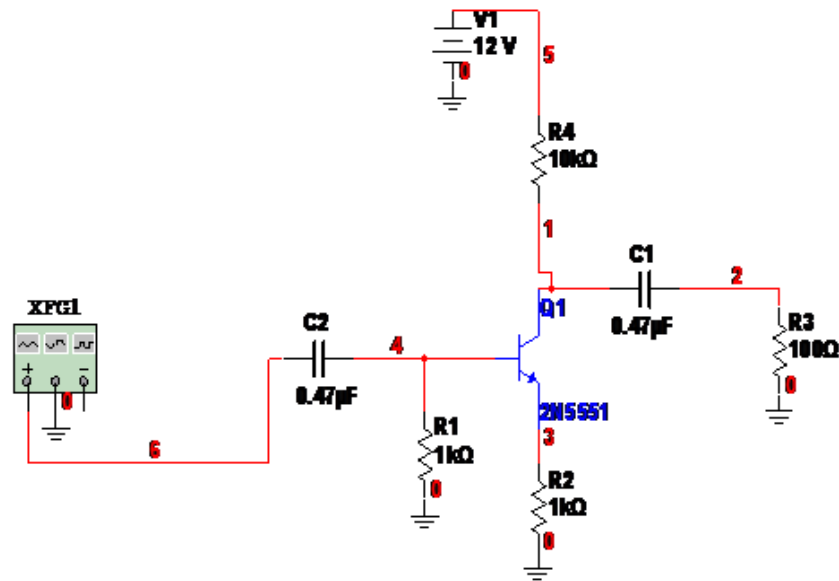


Figure 3.5: UWB pulse Generator using avalanche transistor

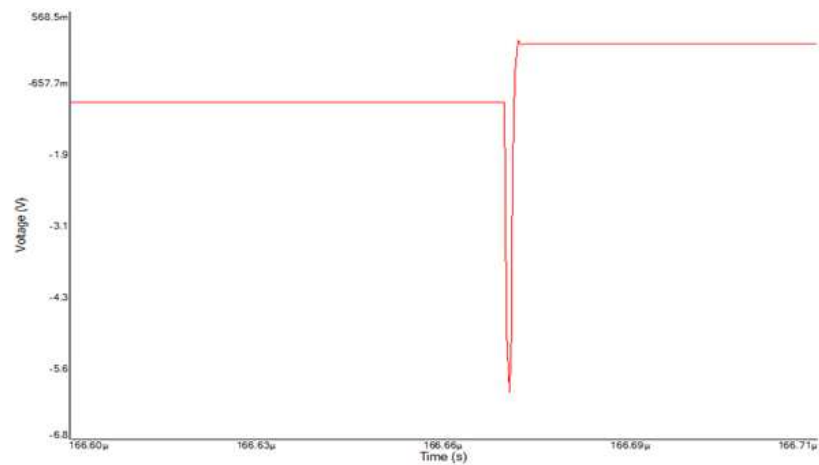


Figure 3.6: simulated output of avalanche circuit

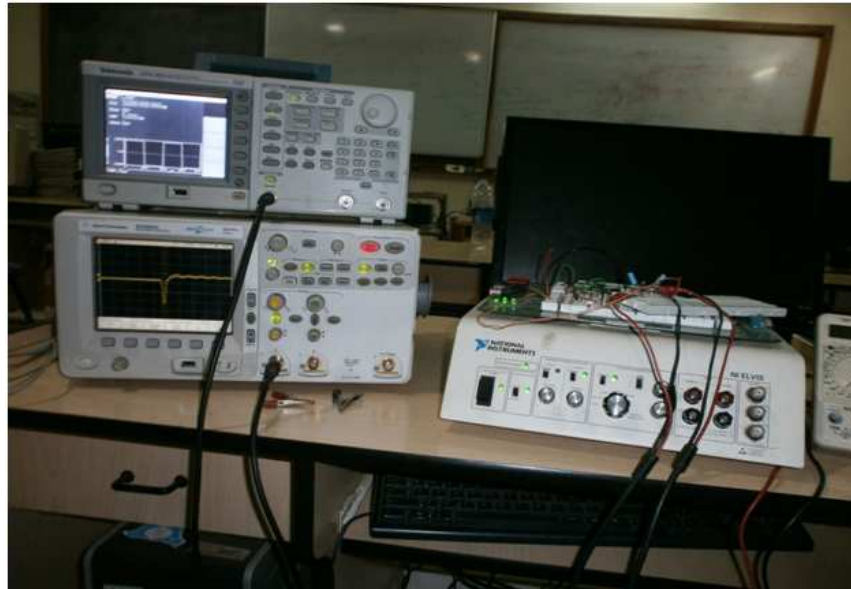


Figure 3.7: Bench setup of the circuit

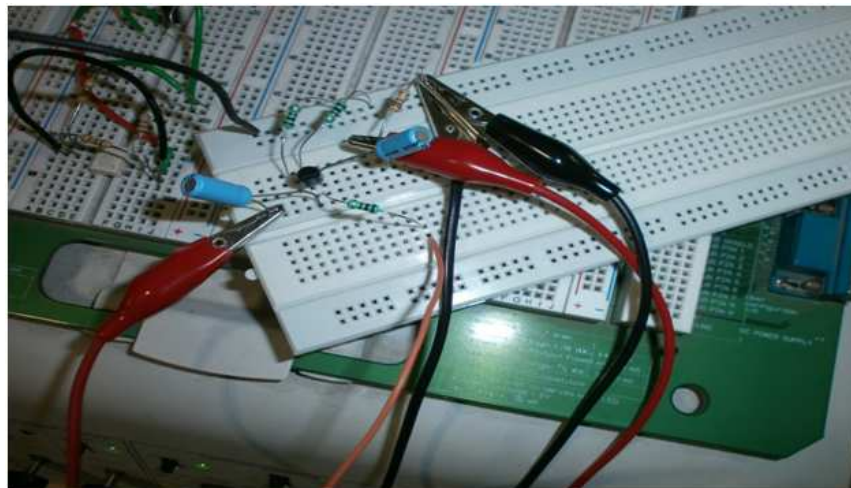


Figure 3.8: Implemented circuit

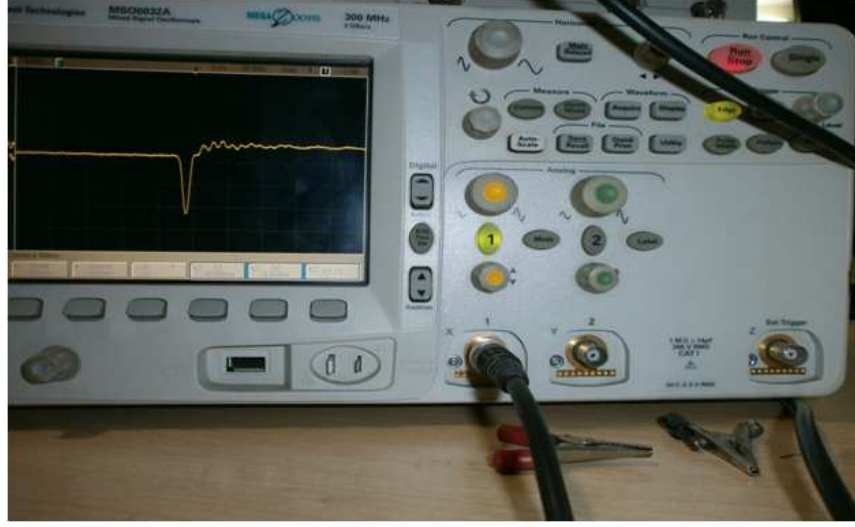


Figure 3.9: Output of the implemented circuit

Parameter	Simulated	Practical on Bread board	Practical on Soldering
Amplitude	-4.97V	-4.47V	-4.47V
Rise Time	0.8ns	6ns	14.5ns
Pulse Width	2ns	11ns	19ns

Table 3.2: Summary of Avalanch Transistor Based UWB pulse generator circuit

11ns duration Gaussian pulse. The practical results is not achieved the simulated results, so we soldered the circuit and checked the output. The soldered circuit is giving 19 ns duration Gaussian pulse.

### 3.3.1 Conclusion

In this work we presented a low complexity and low UWB pulse generator architecture suitable for UWB GPR applications. The circuit provides a Gaussian pulse when activated by a square wave signal from signal generator. Here we used 3 kHz square wave input signal to generate Gaussian pulse. The simulated results are given 2ns duration Gaussian pulse ,but the practical results on breadboard given 11ns duration Gaussian pulse and the practical results on soldering circuit given 19 ns duration Gaussian pulse. Here we demonstrated the Gaussian pulse generation with reduced ringing levels, and good symmetry.

# Chapter 4

## Summary and Conclusion

### 4.1 Summary

In the UWB GPR transmitter, UWB pulse generation is one of the most critical function. There are many techniques are there in the literature to generate UWB pulse. In this project work we have implemented two simple circuits based on the transistors to generate UWB pulse. The first circuit is based on normal transistors and the second circuit is based on the avalanche transistor. Both the circuits are implemented on the bread board and tested with the signal generator and oscilloscope. There is a difference between the simulated results and practical results. For the better result we soldered the circuit in a PCB and verified the result. The output of the PCB differed a lot compare to the expected simulated outcome.

### 4.2 Scope of the future work

Simulated and practical results are quite differed. A excessive theoretical analysis may help us to understand this discrepancies. Simulation with other softwares may help us to understand more. Simulation with more practical cases may gives the comparable results. And Testing with more precise instruments may give good result. Good soldering may be give the simulated results.



## 4.3 Conclusion

UWB pulse generator is important block to realize high resolution GPR. In this research work we have realized two pulse generators based on simple circuits. These circuits are simple, less weight and cost effective. The generated pulse are not meeting the UWB spec requirements. There are Requirements of high quality research in UWB pulse generator with the help of simulation tools as well as sophisticated instruments. Any breakthrough to achieve cost effective, efficient and reliable UWB pulse generator will have huge impact to transform the present generation pulsed GPR technology.

# Bibliography

- [1] Federal Communications Commission et al. Revision of part 15 of the commission's rules regarding ultra-wideband transmission systems. *First Report and Order, FCC*, 2:V48, 2002.
- [2] John C Cook. Status of ground-probing radar and some recent experience. In *Subsurface Exploration for Underground Excavation and Heavy Construction*, pages 175–194. ASCE, 1974.
- [3] John C Cook. Radar transparencies of mine and tunnel rocks. *Geophysics*, 40(5):865–885, 1975.
- [4] David J Daniels. Ground penetrating radar. Institution of Electrical Engineers, 2004.
- [5] AHMED El-Gabaly. Pulsed rf circuits for ultra wideband communications and radar applications. 2011.
- [6] HULSENBECK et al, 1926.
- [7] S Evans. Radio techniques for the measurement of ice thickness. *Polar Record*, 11(73):406–410, 1963.
- [8] Jorge R Fernandes and David Wentzloff. Recent advances in ir-uwband transceivers: An overview. In *Circuits and Systems (ISCAS), Proceedings of 2010 IEEE International Symposium on*, pages 3284–3287. IEEE, 2010.
- [9] Jeongwoo Han and Cam Nguyen. A new ultra-wideband, ultra-short monocycle pulse generator with reduced ringing. *Microwave and Wireless Components Letters, IEEE*, 12(6):206–208, 2002.
- [10] Jeongwoo Han and Cam Nguyen. Ultra-wideband electronically tunable pulse generators. *Microwave and Wireless Components Letters, IEEE*, 14(3):112–114, 2004.

- [11] Prasad K Kadaba. Penetration of 0.1 ghz to 1.5 ghz electromagnetic waves into the earth surface for remote sensing applications. In *Engineering in a Changing Economy*, volume 1, pages 48–50, 1976.
- [12] Jeong Soo Lee and Cam Nguyen. Novel low-cost ultra-wideband, ultra-short-pulse transmitter with mesfet impulse-shaping circuitry for reduced distortion and improved pulse repetition rate. *Microwave and Wireless Components Letters, IEEE*, 11(5):208–210, 2001.
- [13] Jeong Soo Lee and Cam Nguyen. Uniplanar picosecond pulse generator using step-recovery diode. *Electronics Letters*, 37(8):504–506, 2001.
- [14] Jeong Soo Lee, Cam Nguyen, and Tom Scullion. New uniplanar subnanosecond monocycle pulse generator and transformer for time-domain microwave applications. *Microwave Theory and Techniques, IEEE Transactions on*, 49(6):1126–1129, 2001.
- [15] Rexford M Morey. Continuous subsurface profiling by impulse radar. In *Subsurface Exploration for Underground Excavation and Heavy Construction*, pages 213–232. ASCE, 1974.
- [16] BY NILSSON. Two topics in electromagnetic radiation field prospecting. *Dissertation abstracts international. C. European abstracts*, 44(3), 1983.
- [17] A Reizenzahn, T Buchegger, D Scherrer, S Matzinger, S Hantscher, and CG Diskus. A ground penetrating uwb radar system. In *Ultrawideband and Ultrashort Impulse Signals, The Third International Conference*, pages 116–118. IEEE, 2006.
- [18] KC Roe and DA Ellerbruch. Development and testing of a microwave system to measure coal layer thickness up to 25 cm. Technical report, National Bureau of Standards, Boulder, CO (USA). Electromagnetic Fields Div., 1979.
- [19] Bart Scheers. Ultra-wideband ground penetrating radar with application to the detection of anti personnel landmines. *Chapter*, 7:867–871, 2001.
- [20] Alexandre Serres, Yvan Duroc, Tan-Phu Vuong, Jose Ewerton P de Farias, and Glausco Fontgalland. A new simple uwb monocycle pulse generator. In *Electronics, Circuits and Systems, 2006. ICECS'06. 13th IEEE International Conference on*, pages 1212–1215. IEEE, 2006.

- 
- [21] Merrill I Skolnik. An introduction to impulse radar. Technical report, DTIC Document, 1990.
  - [22] Bernard Owen Steenson. *Radar methods for the exploration of glaciers*. PhD thesis, California Institute of Technology, 1951.
  - [23] RR Unterberger. Radar and sonar probing of salt. *The Northern Geological Society*, 1979.
  - [24] Cemin Zhang and Aly E Fathy. Reconfigurable pico-pulse generator for uwb applications. In *Microwave Symposium Digest, 2006. IEEE MTT-S International*, pages 407–410. IEEE, 2006.